

Electronic Supplementary Information for

**Controllable Growth of $\text{Ni}_x\text{Co}_y\text{Se}$ Films and the Composition Influence on the
Photovoltaic Performance of Quasi-Solid-State Dye-Sensitized Solar Cells**

Zhitong Jin, Guanyu Zhao and Zhong-Sheng Wang*

Department of Chemistry, Shanghai Key Laboratory of Molecular Catalysis and Innovative Materials, Laboratory of Advanced Materials, Collaborative Innovation Center of Chemistry for Energy Materials (iChEM), Fudan University, 2205 Songhu Road, Shanghai 200438, P. R. China.

* Corresponding author: E-mail: zs.wang@fudan.edu.cn

Table S1. The power conversion efficiency of DSSCs with multinary metal selenides CEs reported in the literatures.

CEs	Morphology	Liquid electrolyte	PCE/%(Pt)	Ref.
Cu_2SnSe_3	Nanoparticles	I/I_3^-	7.75(7.21)	26
$\text{Ni}_{0.9}\text{Sn}_{0.1}\text{Se}_2$	Nanoparticles	I/I_3^-	4.20(6.11)	27
$\text{Ni}_{0.5}\text{Co}_{0.5}\text{Se}$	Nanocrystals	I/I_3^-	6.02(6.11)	28
$\text{Ni}_{0.33}\text{Co}_{0.67}\text{Se}$	Dandelion-like microspheres	I/I_3^-	9.01(8.30)	29
$\text{Co}_{0.42}\text{Ni}_{0.58}\text{Se}$	Nanosheets and nanoparticles	I/I_3^-	6.15(5.53)	30
NiCoSe	Hollow microspheres	I/I_3^-	9.04(8.07)	31
$\text{Cu}_2\text{ZnSnSe}_4$	Nanoparticles	I/I_3^-	3.85(4.03)	32
$\text{Cu}_2\text{ZnSnSe}_4$	Nanocrystal	I/I_3^-	7.82(7.56)	33
$\text{Cu}_2\text{ZnSnSe}_4$	Nanocrystals	I/I_3^-	7.06(7.43)	34
CuCoSe	Nanosheets	I/I_3^-	7.81	35
CuFeSe		I/I_3^-	7.22	35

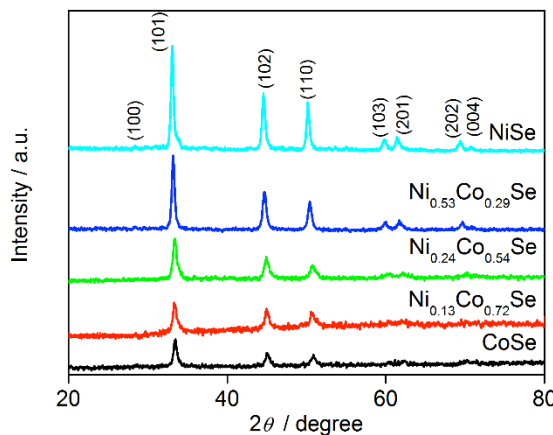


Figure S1. XRD patterns of the precipitate samples.

Table S2. Element ratio (Ni:Co:Se) of as-prepared samples

Feed ratio (Ni:Co:Se)	Ni:Co:Se (Precipitate samples)	Ni:Co:Se In-situ-growth films
0.5:2.5:4	0.13:0.72:1	0.07:0.91:1
1:2:4	0.24:0.54:1	0.12:0.80:1
2:1:4	0.53:0.29:1	0.29:0.63:1

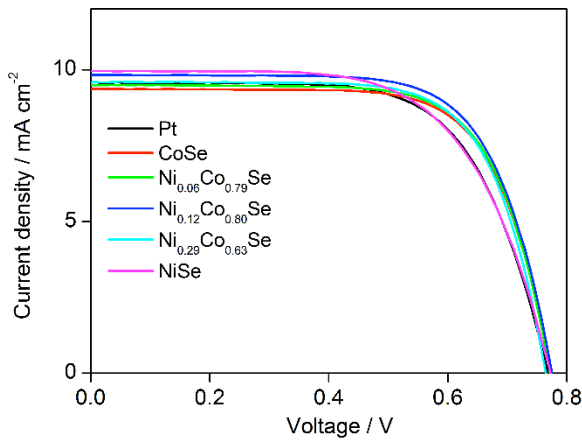


Figure S2. $J-V$ curves of QSDSSCs with Pt, CoSe, NiSe and Ni_xCo_ySe CEs using 5 μm thick TiO_2 films.

Table S3. Photovoltaic performance parameters of QSDSSCs with various CEs using 5 μm thick TiO_2 films.

CE	V_{oc} / mV	J_{sc} / mA cm $^{-2}$	FF	PCE / %
Pt	767	9.58	0.66	4.87
CoSe	772	9.36	0.7	5.11
$Ni_{0.07}Co_{0.91}Se$	771	9.50	0.71	5.16
$Ni_{0.12}Co_{0.80}Se$	775	9.83	0.71	5.32
$Ni_{0.29}Co_{0.63}Se$	764	9.60	0.70	5.17
NiSe	771	9.95	0.64	4.88

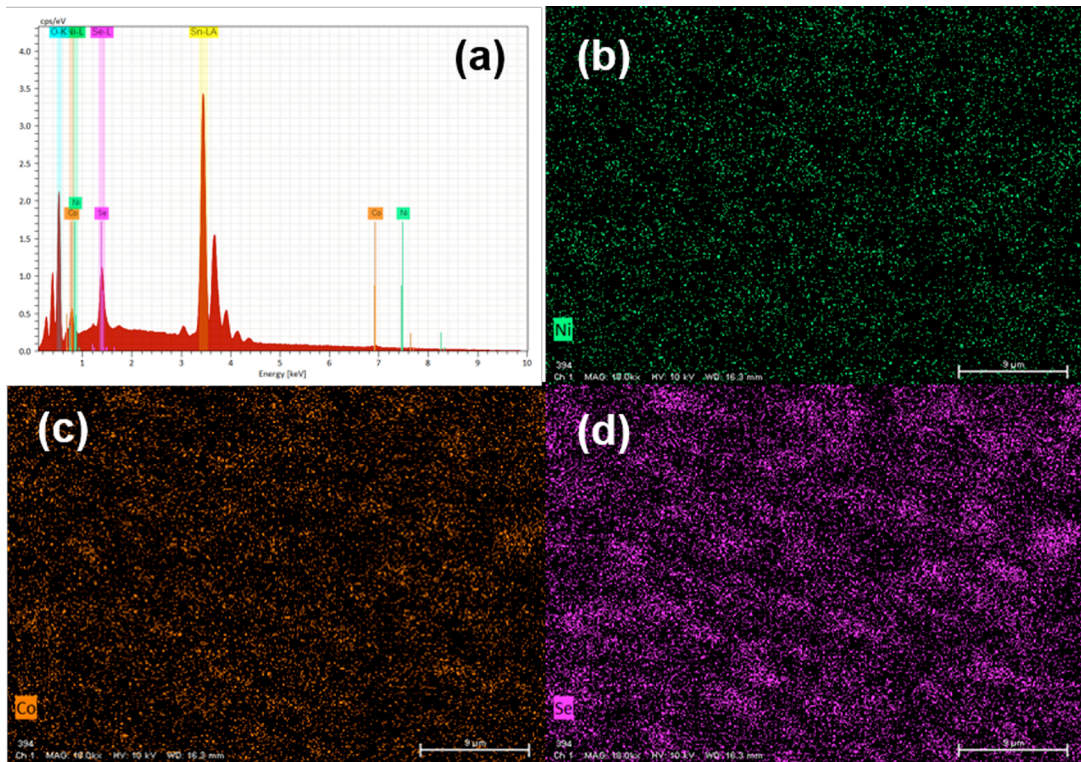


Figure S3. EDS spectrum (a) for $Ni_{0.12}Co_{0.80}Se$ nanoparticles on FTO and SEM-EDS elemental mapping of Ni (b), Co (c), Se (d).

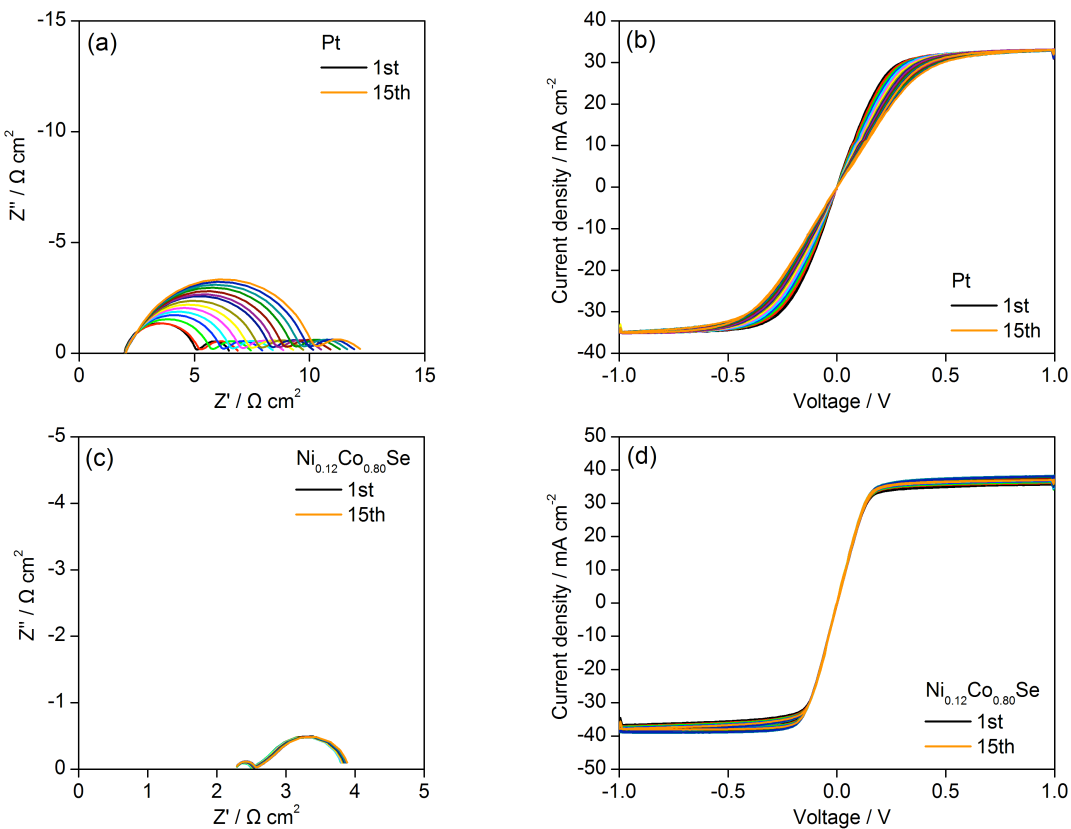


Figure S4. Nyquist plots of EIS and CV plots for the symmetrical cells with Pt (a, b) and $\text{Ni}_{0.12}\text{Co}_{0.80}\text{Se}$ (c, d) CEs, respectively. The cell was first subjected to CV scanning from 0 to 1 V and then from -1 to 0 V with a scan rate of 100 mV s^{-1} , followed by 20 s relaxation at 0 V, and then EIS measurement at 0 V from 0.1 Hz to 300 kHz was performed. This sequential electrochemical test was repeated for 15 times.

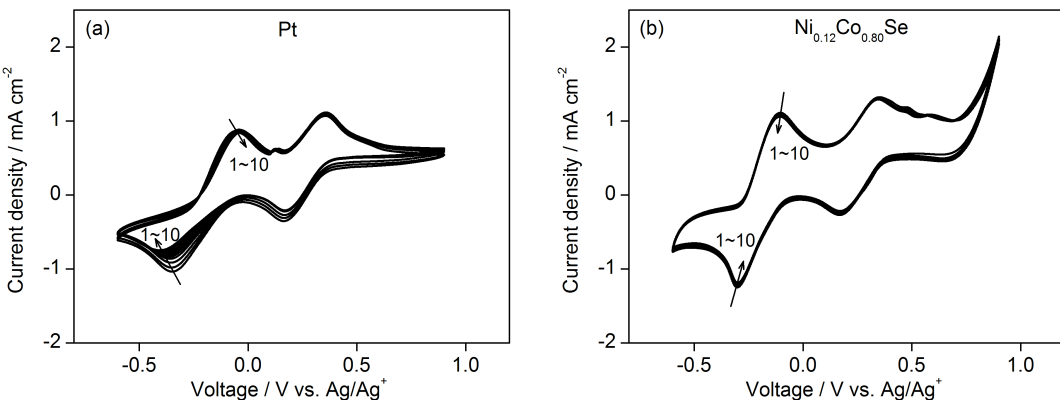


Figure S5. 10-cycle CV curves of (a) Pt and (b) $\text{Ni}_{0.12}\text{Co}_{0.80}\text{Se}$ electrodes in the acetonitrile electrolyte containing 0.1 M LiClO_4 , 10 mM LiI , and 1 mM I_2 for the three-electrode configuration.